Sustainable Environment Research

RESEARCH

Open Access

Biochar-promoted methane production and mitigation of acidification during thermophilic anaerobic co-digestion of food waste with crude glycerol: comparison with re-inoculation

Xiaojue Li[1] and Naoto Shimizu[2*]

Abstract

Food waste and crude glycerol were anaerobically co-digested for 100 days at 52 ± 1 °C with an organic loading rate of 1.0 g L^{-1} d^{-1}. This long-term thermophilic anaerobic digestion (AD) system encountered severe inhibition from volatile fatty acids (VFAs). The study investigated the impacts of re-inoculation (RI) and biochar addition (BA) on this AD process, and monitored the variation of pH, VFAs, total alkalinity and total ammonia nitrogen during treatment. RI treatment was effective in the short term by recovering reactivity after inhibited sludge was mixed 1:1 with active inoculant. In the long term, RI could not reverse process imbalance and finally failed on day 56. Superior performance in methane production and process stability was observed in BA reactors when compared with control and RI reactors. Overall, the biochar contributed to alkalinity and facilitated the activation of methanogenesis and stimulated the conversion of VFAs.

Keywords Biochar, Re-inoculation, Anaerobic co-digestion, Food waste, Crude glycerol

1 Introduction

With the continued rapid growth of the world economy and the human population, the accumulation of food waste (FW) has increased dramatically in the past few years. Every year, one third of the world's food production (about 1,300 Mt) is lost or wasted in the food supply chain, which includes the areas of food production, processing, distribution, storage, retail, and cooking [1]. FW is an easily biodegradable biomass with high water content, and bioconversion is the main method used to simultaneously reduce FW mass and achieve bio-energy recovery. To achieve sustainable development goals, it is necessary to increase the supply of renewable energy and develop methods to stabilize production [2]. Anaerobic digestion (AD) has been proposed as a relatively cost-effective renewable energy production technology for FW management.

Many studies of AD have shown that methane production can be increased by the addition of easily digestible co-substrates, such as readily available and inexpensive crude glycerol (CG) from biodiesel manufacturing [3]. The production of 100 kg of biodiesel will produce approximately 10 kg of impure glycerol, which contains 55–90% glycerol. Compared with other

*Correspondence:
Naoto Shimizu
shimizu@agr.hokudai.ac.jp
[1] Graduate School of Agriculture, Hokkaido University, Sapporo 060-8589, Japan
[2] Research Faculty of Agriculture/Field Science Center for Northern Biosphere, Hokkaido University, Sapporo 060-8589, Japan

co-substrates (agricultural waste, livestock manure), CG has the advantages of easy digestion and long-term storage. In previous research [4], we confirmed that FW co-digestion with 10% (w/w) CG based on volatile solids (VS) proportion improved methane production because of the decomposability and supplementation of the carbon source. However, the accumulation of volatile fatty acids (VFAs), especially propionic acid, in the reactor is recognized as an obstacle to long-term stable operation of AD systems.

VFA inhibition is generally considered to be the main factor affecting the stability of the AD process. Specifically, accumulation of VFAs causes a sharp drop in pH that may lead to loss of activity of acid-sensitive glycolytic enzymes [5] and subsequent reduction in methane production. VFA inhibition appears to be a common problem in long-term AD systems, especially in systems that deal with easily acidified substrate like FW within which the VFA concentration can reach up to 20 g L^{-1} [6]. This limitation hinders the application of AD technology in waste treatment. In addition to low methane production, ammonia suppression is always accompanied by obvious accumulation of VFAs [7]. In recent years, many measures have been proposed to avoid VFA inhibition in AD and to develop efficient and stable AD technology to optimize operating parameters to achieve sustainable goals.

Re-inoculation (RI) with active inoculant is a kind of traditional method to improve digestion efficiency. In previous studies of AD using high solids concentration of rice straw [8], RI was necessary to improve the conversion efficiency of the system and to alleviate the problem of VFA accumulation. Fdez-Guelfo et al. [9] showed that a new RI and start-up of the AD process are required to restore biomethanization performance of a reactor destabilized by a wash-out. Mixing the inhibited sludge with a proportion of active inoculant was also utilized to lower the concentration of long-chain fatty acids (LCFAs) for recovery of mesophilic AD of de-oiled grease trap waste [10]. However, there are few studies on the recovery of thermophilic AD fed by FW and CG.

Alkaline substances are commonly added to VFA inhibition and adjust the pH. However, use of large amounts of alkaline additives can cause microbial inhibition [11] and impose significant costs in long-term AD processes. Biochar is an inexpensive carbonaceous material that was recently identified as a sustainable alternative to commercial-grade carbon-based sorbents for use in AD [12]. Given the ready availability of biochar and its properties of large specific surface area, high microporosity, and strong ion exchange capacity, this material has broad application prospects in environmentally sensitive processes [13]. Although research into biochar applications has increased in recent years, there are still knowledge gaps in the use of biochar in AD processes because complex biochar properties, such as elemental composition (P, Ca, Mg, K, etc.) and functional groups (hydroxyl, amine and carboxylic groups, etc.), depend on different production parameters. In this study, RI and biochar addition (BA) were used as recovery strategies for an easily acidified thermophilic anaerobic fermentation system fed with FW and CG. The effects of RI and BA on anaerobic reactor performance and the properties of the digestate were investigated and compared.

2 Materials and methods

2.1 Inoculant and substrates for AD process

Seed sludge used as inoculant was collected from experiment farm (field science center for northern biosphere, Hokkaido University) which equipped with dairy farming production and AD related facilities, and was held at 52 °C. FW (3.8% protein, 1.9% lipid, 16.1% carbohydrate, 0.7% salt) was obtained from the central restaurant of Hokkaido University. The FW was minced, homogenized using a blender, and then stored at − 4 °C before use. CG derived from the transesterification process during biodiesel production was provided by Revo International Company (Kyoto, Japan). Table 1 lists the main characteristics [total solids (TS), VS, pH, VFA, and total ammonia nitrogen (TAN)] of the substrates and inoculants.

Table 1 Characteristics of food waste (FW), crude glycerol (CG), and inoculants used in this study

	TS [%w.b.][a]	VS [%w.b.]	pH	VFA (mg L^{-1})	TAN (mg L^{-1})
FW	19.70 ± 0.17	17.50 ± 0.16	ND[b]	ND	ND
CG	84.51 ± 0.12	79.82 ± 0.14	8.6	ND	ND
Inoculant 0[c]	2.17 ± 0.62	1.40 ± 0.40	8.0	923 ± 13	1,725 ± 23
Inoculant 1[d]	2.16 ± 0.45	1.49 ± 0.38	8.0	854 ± 19	1,649 ± 42
Inoculant 2[d]	2.57 ± 0.14	1.31 ± 0.09	8.2	823 ± 40	1,707 ± 84
Inoculant 3[d]	2.59 ± 0.11	1.43 ± 0.10	8.2	948 ± 47	1,590 ± 46
Inoculant 4[d]	2.36 ± 0.06	1.69 ± 0.78	8.1	829 ± 6	1,516 ± 37
Inoculant 5[d]	2.56 ± 0.20	1.42 ± 0.22	8.2	864 ± 18	1,579 ± 73
Inoculant 6[d]	2.28 ± 0.21	1.48 ± 0.15	8.1	868 ± 41	1,457 ± 18
Inoculant 7[d]	2.98 ± 0.07	1.75 ± 0.07	8.2	864 ± 24	1,442 ± 45
Inoculant 8[d]	2.80 ± 0.40	1.46 ± 0.44	8.1	842 ± 21	1,436 ± 17
Inoculant 9[d]	2.63 ± 0.14	1.41 ± 0.13	8.2	875 ± 40	1,500 ± 55

[a] % Wet basis

[b] Not determined

[c] Inoculant used for initial AD experiments

[d] Inoculant used for each re-inoculation

2.2 Biochar preparation

Wood chips of conifer trees (*Abies sachalinensis*) from northern Hokkaido were used as feedstock for biochar production. The wood chips were dried in a drying oven (Isuzu Seisakusho, Niigata, Japan) at 105 °C for 24 h before grinding. Powdered raw samples were passed through a 2-mm sieve. Biochar was produced by heating powdered feedstock in covered crucible containers in a muffle furnace (FO810; Yamato Scientific, Tokyo, Japan) under oxygen-limiting conditions at a pyrolytic temperature of 600 °C. The heating rate was set at 10 °C min^{-1}, and the residence time was 3 h. The biochar samples were allowed to cool to room temperature in the muffle furnace and were stored in airtight plastic bags prior to use.

2.3 AD condition and recovery strategies

According to our previous experimental results [4], FW and CG were mixed in a ratio of 9:1 (based on the weight of VS provided) for use as feed material. Schott Duran bottles (1.0 L total volume; 0.9 L working volume) with rubber stoppers were used as anaerobic testing reactors. Feed was added once a day with an organic loading rate of 1.0 g VS L^{-1} d^{-1}. All reactors were inoculated with 0.2 L of inoculant, capped after flushing with nitrogen for 3 min to remove oxygen, and kept in an incubator (MIR-153; SANYO Electric, Osaka, Japan) at 52 °C.

To test the effects of RI and BA as recovery strategies, one treatment group without any recovery strategy was set as the control. The RI strategy involved the RI of the digestate in a 1:1 ratio with fresh inoculant, 0.1 L of effluent from the reactors were replaced by an equal volume of fresh inoculant (the characteristics of inoculant added at each phase are shown in Table 1) to supplement the methanogenic population, whereas the BA strategy involved the addition of 2.0 g of biochar to the reactor in each phase [hydraulic retention time (HRT) of 10 d]. For each strategy, the respective treatment (RI or BA) was conducted only once each phase. Throughout each treatment, feeding of the digester continued for the entire operating period and the loading conditions were kept consistent with the control group. The detailed operating conditions and experimental designs are presented in Fig. 1. The entire anaerobic fermentation experiment was carried out in ten phases with a full duration of 100 days. All groups were carried out in quadruplicate, with three reactors used only for recording biogas production and composition analysis, and one for digestate analysis.

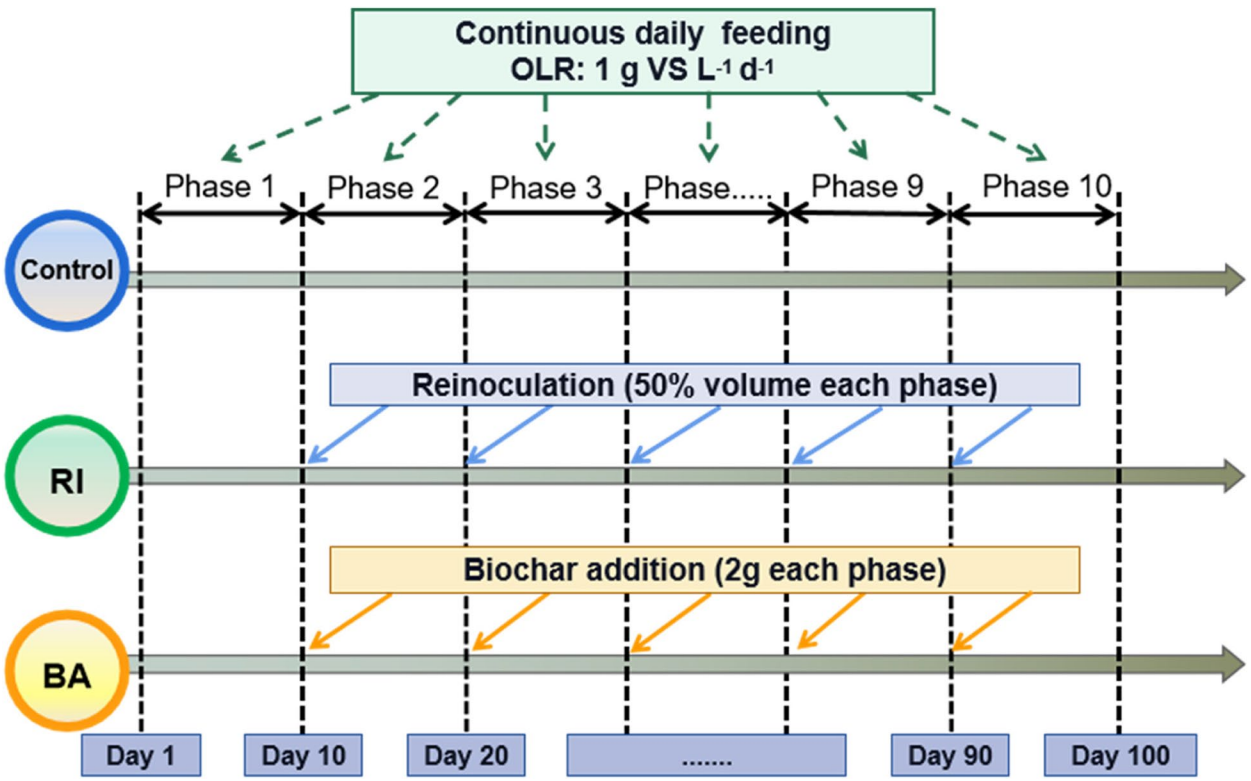

Fig. 1 Graphical representation of operating conditions and experimental design

2.4 Analytical methods

2.4.1 Methane quantification

Generated biogas was collected in gas bags and its volume was measured using a wet gas meter (W-NK; Shinagawa, Tokyo, Japan). The methane content of the produced biogas was measured using a gas chromatograph (GC-4000; GL Science, Tokyo, Japan) with a flame ionization detector. Biogas production and its composition were checked daily. The biogas volume was normalized (T = 0 °C, P = 105 Pa) according to Eq. (1):

$$V_N = \frac{V \times 273 \times (760 - P_w)}{(273 + T) \times 760} \quad (1)$$

where V_N is the volume of the gas under standard conditions (normal liters, NL), V is the volume of the biogas (NL), P_w is the water vapor pressure as a function of ambient temperature (mm Hg), and T is the ambient temperature (°C).

In this study, evaluation of methane production was based on corrected methane yields according to standard temperature and pressure. Curve fitting of the values of methane production was based on the modified Gompertz model [14] shown in Eq. (2):

$$H = P \times \exp\left\{-\exp\left[\frac{R_m e}{P}(\lambda - t)\right] + 1\right\} \quad (2)$$

where H is the cumulative methane production (NL) recorded at time t (d); P is the methane potential (NL); R_m is the maximum methane production rate (L d^{-1}); e is exp (1) = 2.718; and λ is the lag-phase period (d). The fitness of this model was evaluated using analysis of variance and significance was based on a 95% confidence level.

The methane accumulation over 100 days of AD was recorded and used for determining the kinetic constants of all reactors. The dynamic process was then simulated, and the methane production potential of all groups was quantitatively analyzed. The fitting of this model was performed using Origin 2020b software (OriginLab, Northampton, MA, USA).

2.4.2 Characteristics of digestate

Digestate samples were collected from the anaerobic digesters each day to study the physicochemical properties. TS, VS, and total alkalinity were determined according to Standard Methods [15]. pH was measured using a pH meter (pH Testr30; Takemura, Tokyo, Japan). The concentrations of VFAs and TAN were assessed by a titration method using a Type B-323 Distillation Unit (BUCHI, Tokyo, Japan). The VFA components in the digestate were analyzed by high-performance liquid chromatography (HPLC, 1260 Infinity; Agilent, Santa Clara, CA, USA) equipped with a Shodex RSpak KC811 column (Showa Denko, Tokyo, Japan). Elution was performed with 0.1% H_3PO_4 as mobile phase at a flow rate of 0.9 mL min^{-1}. The column temperature was maintained at 40 °C and separation was monitored by refractive index detection. All liquid samples were collected in duplicate and were filtered through a 0.45-μm polytetrafluoroethylene membrane filter before injection to the HPLC.

2.4.3 Characterization of the biochar before and after AD

The surface morphology of the biochar was observed using a field-emission scanning electron microscope (SEM, JSM-6301F; JEOL, Tokyo, Japan). The biochar samples were dried at 35 °C for 12 h, attached to aluminum stubs with double-sided carbon tabs, and sputtered with gold. The micrographs were captured at an accelerating voltage of 10 kV.

Raw biochar and biochar samples after AD were dried at 105 °C, homogenized, ground, and sieved through a 0.5 mm sieve prior to analysis of X-ray diffraction (XRD) and Fourier transform infrared spectroscopy (FTIR). The XRD patterns of the biochar samples were examined at 40 kV and 30 mA using a high-intensity X-rays generating equipment (Rigaku RINT-2000) with a Cu-K α radiation source. A continuous 2θ scan mode from 15° to 70° with a step size of 0.02° and a scan speed of 1.0° min^{-1} was applied. The phase peaks were identified by comparing the observed XRD patterns with standards compiled by Profex software (v 4.2.0).

FTIR analysis was performed on a JASCO IRT-3000 N spectrometer equipped with an attenuated total reflection (ATR) accessory. The FTIR spectra were recorded from the wavenumber range of 4000–550 cm^{-1} using a combined 128 scans with a resolution of 4 cm^{-1}. The spectrum obtained from the background air in the detection chamber was subtracted from the spectrum of each sample to remove the effects of ambient moisture and CO_2. The broadband chemical groups were assigned according to Tipson [16].

The pH, electrical conductivity (EC) and elemental composition of biochar samples were determined by the Tokachi Federation of Agricultural Cooperatives.

3 Results and discussion

3.1 Variations of methane production, specific methane yield, and VS removal rate

Methane yield is an important indicator in reflecting the efficiency of AD. Figure 2 shows the daily and cumulative methane yields of the control, RI, and BA groups. All groups started normally, and similar daily methane variation was detected during the first phase (0–10 d). The first methanogenesis peak for each reactor was observed

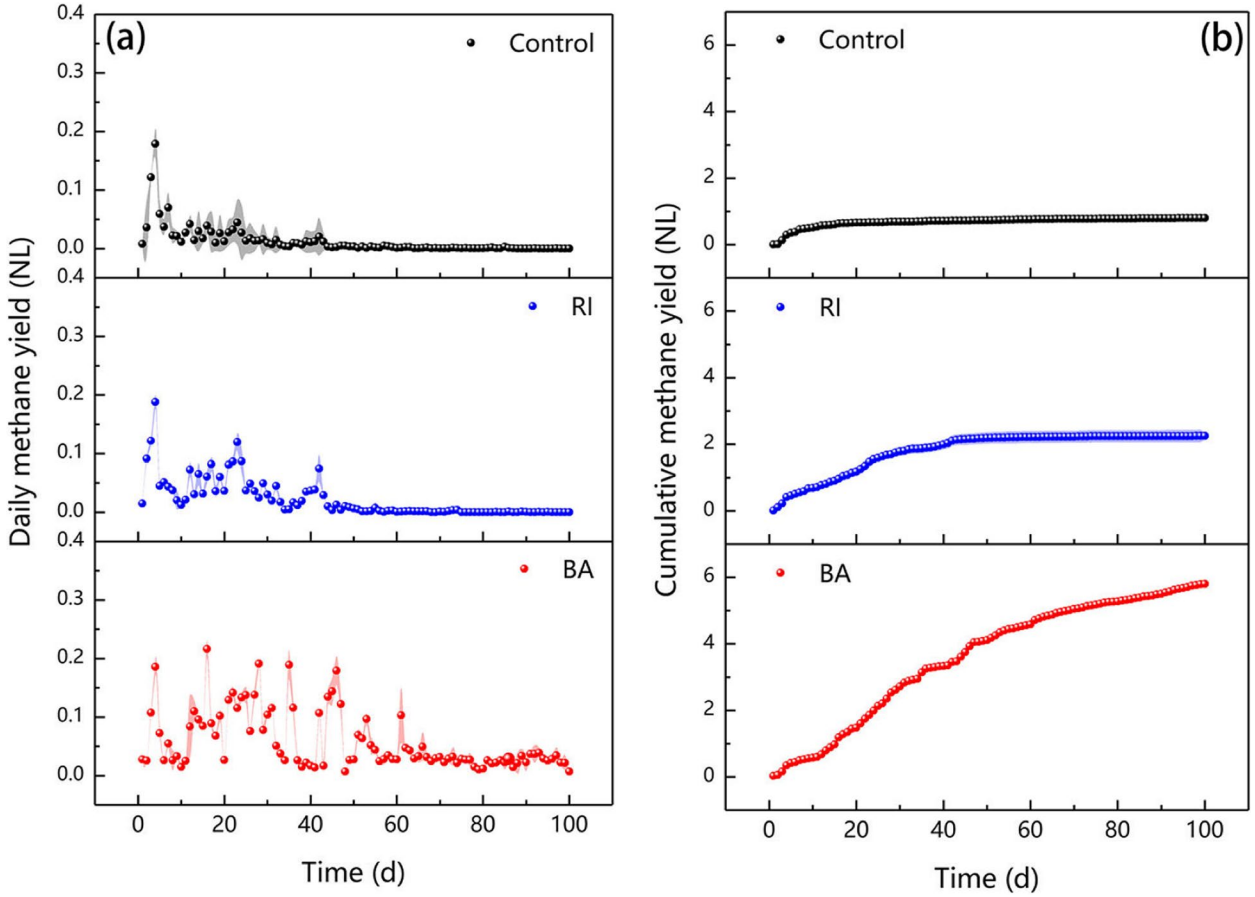

Fig. 2 Daily methane yield (**a**), cumulative methane yield (**b**) of control, RI, and BA group. Shaded areas indicate error bars

during the third day, resulting from the assimilation of readily degradable and dissolved substances into methane. Subsequently, the occurrence, duration, and methane production values differed among all reactors after re-inoculating the RI reactor and adding biochar to the BA reactor. From phase 2 (11–20 d), it was difficult to observe obvious methane production peaks in the control reactors. Strong daily peaks were observed in the RI reactors on day 23 (0.12 NL) and day 42 (0.07 NL), but these peaks were significantly less than those observed in the BA reactors, which showed stable daily peaks (0.10–0.22 NL) during the first 6 phases.

A kinetic study of the cumulative methane production for all reactors during the entire AD process (100 days) was performed using a modified Gompertz model (see Table 2). The lag-phase period (λ) was generally short in the entire experiment process, which may be due to the large amount of carbohydrates contained in feedstocks, which are easily degraded. The methane potential (*P*) for the control reactor was 0.66 NL. For RI and BA reactors, *P* increased to 2.11 and 5.48 NL, respectively. In particular, the methane potential of the BA reactor was nearly three times that of the RI reactor. The values of R_m and *P* showed that RI and biochar addition improved the methane production potential.

Table 2 Gompertz kinetics data for methane production in different experimental reactors

	Gompertz kinetics for biogas production			
	P (NL)	R_m (NL d^{-1})	λ (d)	R^2
Control	0.66 ± 0.01	0.10 ± 0.40 × 10^{-2}	2.61 ± 0.08	0.98
RI	2.11 ± 0.05	0.07 ± 0.20 × 10^{-2}	2.05 ± 0.38	0.98
BA	5.48 ± 0.07	0.12 ± 0.20 × 10^{-2}	7.72 ± 0.29	0.99

In the absence of precise process control and recovery strategies, the high protein and lipid contents in FW, impurities in CG, and propionic acid derived from CG led to inhibitory levels of ammonia, hydrogen sulfide, and LCFAs. These harmful intermediate compounds can be easily generated to cause reduced system stability, low methane yield or foaming. Therefore, under continuous feeding conditions, the methane production performance

of the control reactor declines greatly, and almost no methane can be produced from day 16.

As shown in Fig. 1, the RI reactors were re-inoculated every 10 days to alleviate VFA accumulation and overcome inhibition periods. However, although the RI strategy was effective until day 50, its long-term effect (50–100 days) was weak. After the fourth RI, the daily methane production was significantly lower than that in the first three phases. During the 50- to 100-day period, the RI reactor was no longer able to produce methane, even if RI was performed. Because the effluents from RI reactor effluent consistently exhibited higher VFAs compared to the BA reactor, especially in the latter phase of the experiment. It showed an increasing trend of VFAs concentrations in RI reactors from 50 d, indicating the accumulation of intermediates produced from hydrolysis and acidification during AD. Propionic acid emerged as the main inhibitory VFA during long-term anaerobic co-digestion of FW and CG because propionate oxidation via acetogenesis is a highly endergonic reaction. Also, the self-recovery of the anaerobic micro-ecosystem would take a long time once the anaerobic bacteria were inhibited by VFAs [17]. RI could not fundamentally reverse the process imbalance, but only delayed the process failure by replacing acidified digestate with fresh inoculant, finally, the methanogens could not tolerate the uncontrollable fluctuations of VFAs in RI reactors.

Over the entire AD process, the BA reactor was more effective than the RI reactor because of the consistently higher methane production over the first five phases (0–50 d). In the later stages of AD, the control and RI reactors stopped producing biogas, whereas the BA reactor kept working up to day 100, even though its methane production rate decreased slightly. Higher rates of VS removal generally means that more organic material can be converted to biogas. In the control reactor, the VS removal efficiency reached 53 ± 5% in the first phase, but remained at lower levels (28–47%) in the subsequent phases, indicating accumulation and poor degradation of input material. Compared with RI treatment, the addition of biochar resulted in higher VS removal efficiency in AD treatment of FW and CG, which remained above 50% throughout the trial period.

The specific methane yield (SMY), defined as the amount of methane produced for a given quantity of removed VS, is the result of the activity of anaerobic flora. It depends on the amount of a given carbon substrate under anaerobic respiration conditions, and is also up to the utilization of biodegradable substances for achieving the biogas production potential in the AD process which contains hydrolysis, acidogenic fermentation, hydrogen-producing acetogenesis, and methanogenesis. Complex organic substances are decomposed into soluble monomers by the action of extracellular hydrolytic enzyme of acetogens, and then converted into terminal products, and finally, the acidified products (acetic acid, formic acid, etc.) are converted to methane by strictly anaerobic methanogens [18]. The SMYs of the different reactors were determined for each phase (Table 3). The SMY data for the BA group (0.12–0.56 NL g^{-1} VS) indicates that the unique chemical properties of biochar, such as graphitic, aromatic carbon matrices, phosphorous groups and polycyclic aromatic hydrocarbons (see details in Sec.3.3.2), contributed to methanogenic performance to varying degrees. Yin et al. [19] also found that biochar enhanced VS removal efficiency and methane production by 18 and 25%, respectively, through accelerated electron transfer during substrate consumption by enriching methanogens. Conversely, although the RI group also showed higher VS removal efficiency than the control

Table 3 Specific methane yield, electrical conductivity, and VS removal rate of digestate from different experimental reactors

Phase	Control		RI		BA	
	VS removal efficiency (%)	SMY (NL g^{-1} VS)	VS removal efficiency (%)	SMY (NL g^{-1} VS)	VS removal efficiency (%)	SMY (NL g^{-1} VS)
1	53 ± 5	$0.53 \pm 1.10 \times 10^{-2}$	49 ± 8	0.65 ± 0.07	51 ± 4	0.56 ± 0.01
2	34 ± 5	$0.21 \pm 5.10 \times 10^{-2}$	58 ± 3	0.31 ± 0.02	65 ± 5	0.49 ± 0.04
3	35 ± 8	$0.03 \pm 0.70 \times 10^{-2}$	66 ± 3	0.28 ± 0.01	71 ± 5	0.56 ± 0.04
4	42 ± 3	$0.02 \pm 1.10 \times 10^{-2}$	63 ± 2	0.13 ± 0.01	78 ± 1	0.27 ± 0.01
5	47 ± 6	$0.02 \pm 0.30 \times 10^{-2}$	65 ± 3	0.09 ± 0.01	68 ± 8	0.44 ± 0.05
6	46 ± 1	$0.02 \pm 0.60 \times 10^{-2}$	62 ± 1	$1.40 \times 10^{-2} \pm 0.50 \times 10^{-2}$	68 ± 2	$0.24 \pm 0.20 \times 10^{-2}$
7	45 ± 7	$0.90 \times 10^{-2} \pm 5.92 \times 10^{-2}$	57 ± 4	$0.01 \pm 0.20 \times 10^{-2}$	66 ± 3	0.24 ± 0.03
8	28 ± 4	$0.70 \times 10^{-2} \pm 0.20 \times 10^{-2}$	49 ± 1	$0.70 \times 10^{-2} \pm 0.20 \times 10^{-2}$	61 ± 2	0.13 ± 0.01
9	41 ± 5	$0.01 \pm 0.20 \times 10^{-2}$	35 ± 8	$0.40 \times 10^{-2} \pm 0.20 \times 10^{-2}$	61 ± 3	$0.12 \pm 0.80 \times 10^{-2}$
10	42 ± 3	$0.20 \times 10^{-2} \pm 6.92 \times 10^{-4}$	52 ± 5	$0.20 \times 10^{-2} \pm 3.63 \times 10^{-4}$	56 ± 8	0.17 ± 0.02

group, the consumed VS was not well converted to methane based on SMY values (0.002–0.09 NL g^{-1} VS) after phase 5.

It is also worth noting that the observed results would be attributed to the accumulation of biochar decreasing methane production. The methane production showed a downward trend after 67 d, and the VS removal efficiency also decreased from highest 78 (phase 4) to 56% finally. In a study by Shen et al. [20], no significant difference was observed between both the modified digesters with high dosage of pine biochar (4.97 g g^{-1} dry matter of sludge), white oak biochar (4.40 g g^{-1} dry matter of sludge) and controls in terms of methane volume because the high dosage of biochar possibly inhibited microbial activity and kinetics. This inhibition was more apparent under thermophilic AD compared with mesophilic condition. And according to their response surface methodology modeling, the effect of biochar dosage on the methane content and methane accumulation was more complex during thermophilic AD. Therefore, excessive biochar accumulation over time in the reactors may cause a decline in biomethane production because of the nonselective adsorption behavior of biochar which can easily lead to the immobilization or inactivation of hydrolase, and adsorption of nutrients and useful metabolites before utilization and transformation [21].

3.2 Effects of RI and BA strategies on reactor chemical conditions

One of the core objectives of this study was to determine the effects of RI and BA treatments on AD performance using easily acidified substrates. This approach required the monitoring of pH, VFA, alkalinity and TAN as process performance parameters.

3.2.1 Variation of pH and VFAs in AD reactors

Figure 3 shows the daily variation in pH for the control, RI, and BA treatments. For each treatment, pH was observed to fluctuate in accordance with feed degradation. The initial pH values of the control, RI and BA groups were 8.4, 8.3, and 8.2, respectively. In the initial phase without imposing any additional recovery measures (the first 10 days), similar trends of pH fluctuation were observed for the three groups. The pH of the control group showed a brief recovery on day 23, but afterward it presented a mainly downward trend. As the feeding continued, pH of the control group went through a rapid decline to 5.3 and accompanied with high VFA concentration (5,540–19,300 mg L^{-1}). It is difficult to maintain the neutral pH of the control reactors without the influence of external force due to the rapid acidification of daily feed.

The pH trend of the control reactor suggested that intervention was necessary to prevent acidification of thermophilic anaerobic co-digestion reactors. To ease the acidification trend, 50% of the digestate from the RI reactor was replaced with fresh inoculant and the positive effect of RI was immediately observed. The methane yield and pH were obviously stabilized after the external intervention. From day 10, the pH of the RI and BA reactors recovered to between pH 7.0 and 8.0. The ability of AD to adapt to changes in pH to a stable working range is

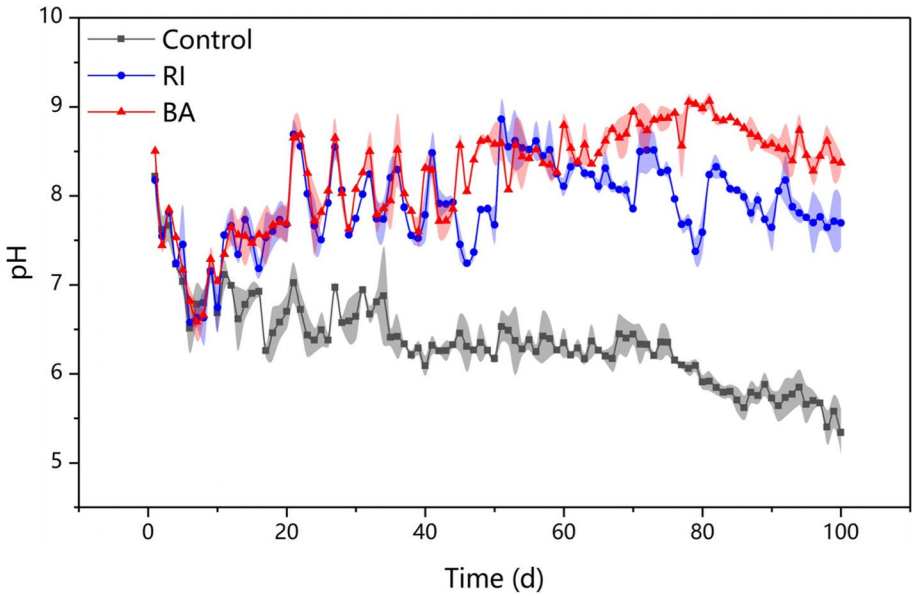

Fig. 3 Variations in pH in different reactors. Shaded areas indicate error bars

known as self-buffering. There were regular fluctuations in pH in the RI and BA reactors from day 20 to day 40, which were attributed to the acclimatization and adaptation of the reactors. However, during the period from day 50 to day 100, the pH of the RI reactor showed a sustained drop after RI until the end of each phase. This means that simple RI of acidified digestate was unable to moderate the destabilized reactors.

It was expected that the pH in BA reactors would increase with biochar addition because of the alkaline nature of biochar (pH = 8.9), which was significantly higher than that of the control. This is mainly attributable to the release of ash-inorganic alkalis, alkaline earth metals (K, Ca, and Mg) and organic alkalis functional groups in biochar [22]. Even with daily feeding with easily acidified substrates, the BA reactors could tolerate high VFA accumulation in the presence of biochar, therefore, the addition of biochar could be an ideal strategy to improve the buffering capacity.

Co-digestive systems exhibit high hydrolysis and acid production because of the high biodegradability of the FW and CG present in such systems. Figure 4 shows the accumulation of VFA and individual acid components in the effluent of the control, RI, and BA reactors. The VFAs (acetic acid, propionic acid, butyric acid, valeric acid) were the core products of acidogenesis in this study. The predominant accumulated VFAs were acetic acid and propionic acid in all three treatments. Similar VFA concentrations were observed in the initial start-up phase with subsequent increased degradation of organic matter from FW and CG as reflected by increasing VFA levels up to day 10. For the control treatment without any recovery strategy, the soluble products continued to accumulate in the reactors during the continuous feeding period and reached its first peak ($16{,}300 \pm 121$ mg L^{-1}) on day 33, thereby resulting in significantly higher VFAs concentration than the other two reactors. High levels of propionic acid accumulation, reaching 5.4 and 4.5 g L^{-1} on days 30 and 40, respectively, were also observed in the control reactor, which reduced the buffering capacity and lowered the pH, thereby weakening the efficiency of the biomethanation process. At the end of AD on day 100, the propionic acid concentration in the control reactor was 5.68 g L^{-1} and seemed to be difficult to be consumed. Propionic and butyric acids are generally considered difficult to oxidize because the process is thermodynamically unfavorable in the absence of hydrogen consumption by methanogens [23]. RI and biochar treatments helped to

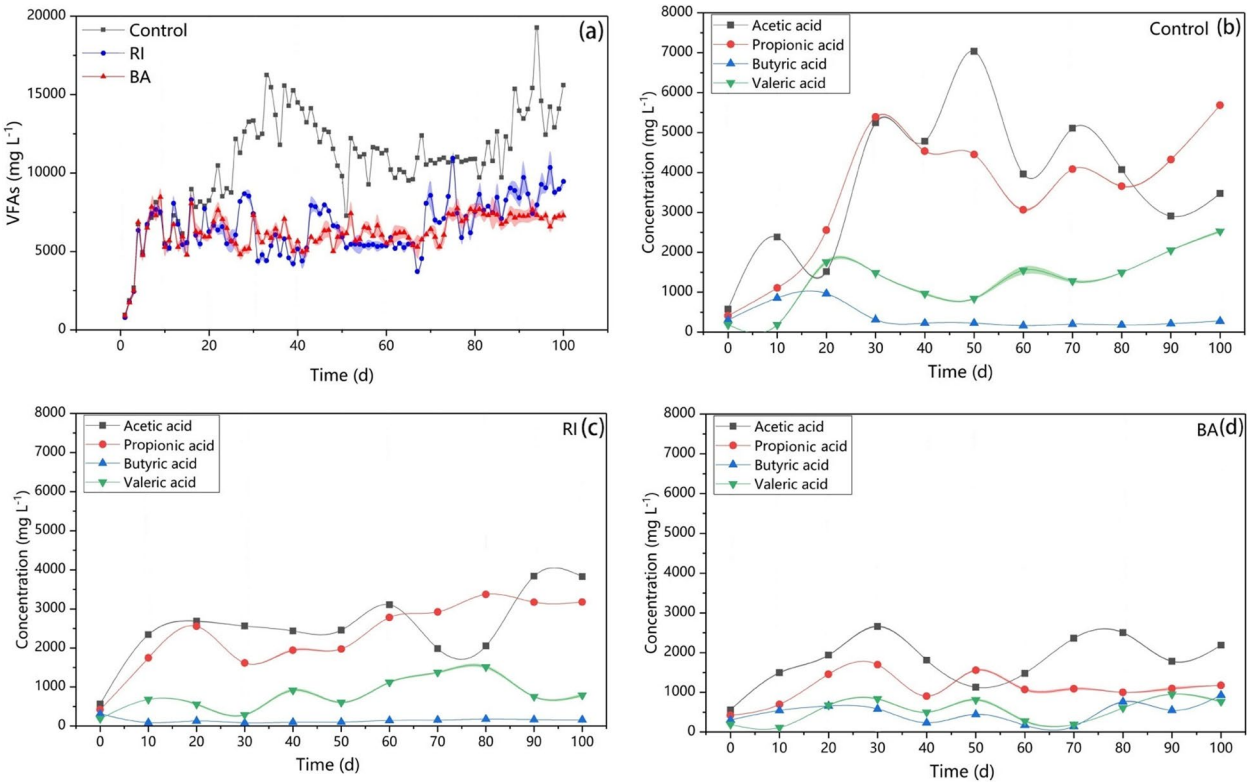

Fig. 4 Variations in VFAs concentrations (**a**) and compositions in different reactors: (**b**) Control reactor; (**c**) RI reactor, and (**d**) BA reactor. Shaded areas indicate error bars

alleviate the accumulation of VFAs, with the BA reactor having lower VFAs concentrations and more effective conversion of propionic acid. In previous research by Xu et al. [24], the secondary accumulation of VFA was also reduced in the AD treatment of sulfate wastewater when mediated by biochar. Generally, in the presence of biochar, the enhanced acetic acid and butyric acid degradation can provide abundant hydrogen for more efficient degradation of propionic acid [25].

3.2.2 Variation of total alkalinity concentration and TAN in AD reactors

The total alkalinity concentrations in the reactors were determined daily (see Fig. 5). The addition of biochar maintained the $CaCO_3$ alkalinity in the BA reactor at a high level of 5000–9000 mg L^{-1}, thus providing buffering capacity for the AD treatment of FW with CG. These results demonstrated the potential benefits of using biochar as an additive to help maintain alkalinity and counter the effects of acidification. Buffering capacity is necessary to alleviate AD reactor instability while the biochar elemental composition, surface organic functional groups, soluble organic compounds, salts of bicarbonate and carbonate will contribute to total alkalinity [26]. Cations of Na, K, Ca, Mg, Fe, organic functional groups, and inorganic basic species in biochar will help the AD system to equilibrate in the BA reactor. Biochar character and composition also contribute to AD performance

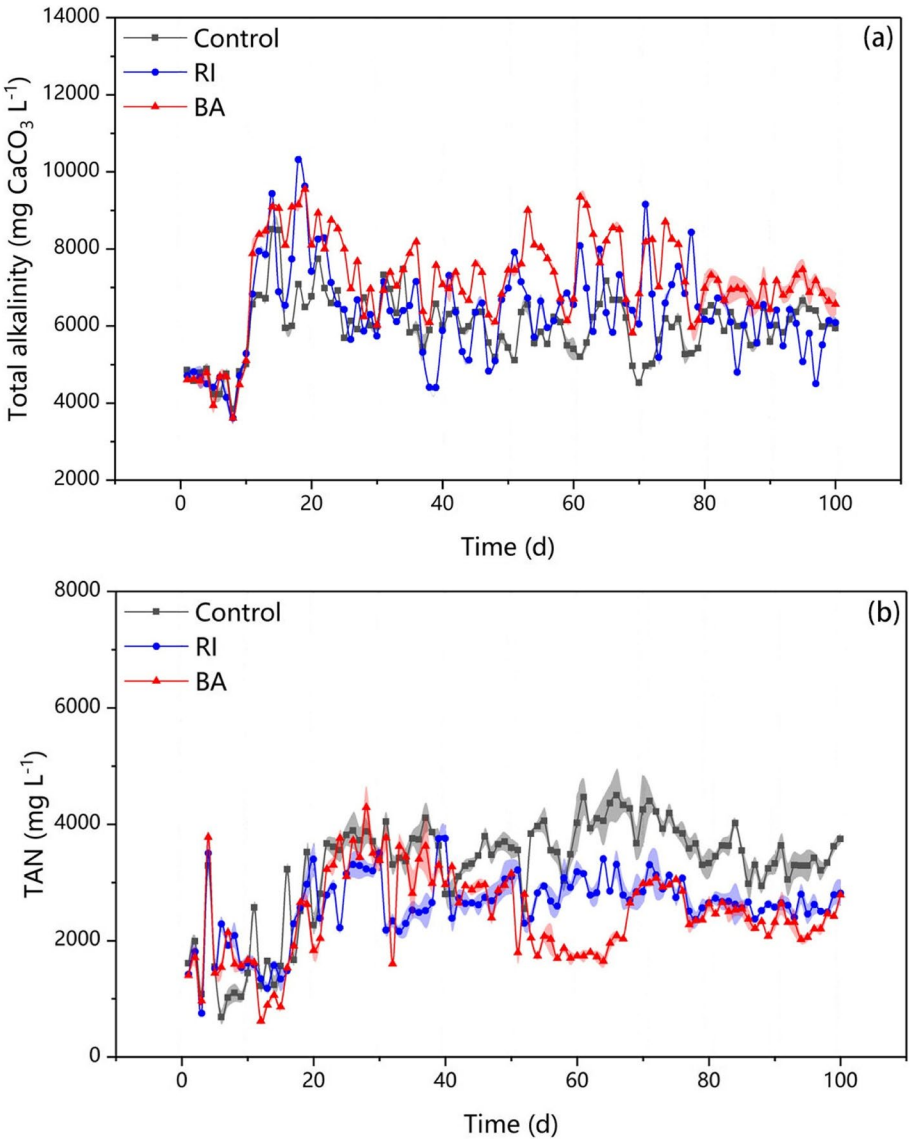

Fig. 5 Variations in the total alkalinity (**a**) and TAN concentrations (**b**) in different reactors. Shaded areas indicate error bars

in terms of biomethanation productivity. This can also be attributed to the microspore surface area of biochar and its relative adsorption properties and pyrolysis temperature to alleviate inhibition and attract microorganisms to its surface.

From day 30, the TAN concentration in the control reactor was noticeably higher than the TAN levels in the RI and BA reactors, which may indicate that the TAN concentration (2,800–4,500 mg L^{-1}) in the digesters was the main driver of total alkalinity. During the AD process, the accumulation of higher ammonium concentrations affected microbial growth rate and metabolic performance and resulted in low methane production. Although TAN ions (NH_3 or NH_4^+) may be toxic to the growth and development of methanogens, biochar reactors maintained favorable pH values (7.5–8.5) at higher TAN concentrations above 2000 mg L^{-1} with no significant inhibitory effect. This may have been caused by the adsorption capacity of individual biochars, which are capable of adsorbing ammonium ions and promoting electron transfer of NH_4^+ with cations on the biochar surface [27]. The BA reactor tolerated TAN concentrations above the recommended ammonia suppression threshold of 1700–1800 mg L^{-1} [28]. This study demonstrates the efficacy of biochar in reducing TAN inhibition and retaining robust reactor performance at higher concentrations. Furthermore, biochar can be used as a suitable additive to control high TAN content while maintaining reactor stability for enhanced energy recovery without increasing environmental risk.

3.3 Characteristics of biochars before and after AD

3.3.1 SEM and compositional analysis

Fagbohungbe et al. [29] proposed that the addition of biochar to AD processes can alleviate substrate-induced instability in three main ways: (1) the adsorption of inhibitors; (2) the increased buffering capacity of AD; and (3) the immobilization of bacterial cells. SEM was used to examine the solid particle morphology of biochar and to provide information on microstructural changes (Fig. 6). Sponge-, honeycomb-, and fence-like porous structures, which originated from the tissue structure in the precursor plants, were observed in the biochar particles. The existence of pores on biochar is important for microbial activities, and the presence of macropores on biochar provides suitable habitats for microbial communities [30].

Table 4 summarizes the pH, EC, ash content, total carbon and nitrogen, nitrate nitrogen and ammonia nitrogen, and elemental composition of biochar before and after AD. The pH of biochar was alkaline (pH 8.9) because of the gradual loss of acidic surface groups and volatile matter at high pyrolysis temperatures [31]. Fe, Ni, Co, Mg, K, and Ca are necessary as supplements to avoid nutritional deficiencies in the AD process [22]. The importance of Fe depends on its redox properties and its role in energy metabolism, where Fe reacts as an electron acceptor and donor in the transport system of methanogenic bacteria to convert CO_2 to CH_4 [32]. Ni and Co are also vital cofactors for carbon monoxide dehydrogenase, acetyl coenzyme-A decarboxylase, and other enzymes

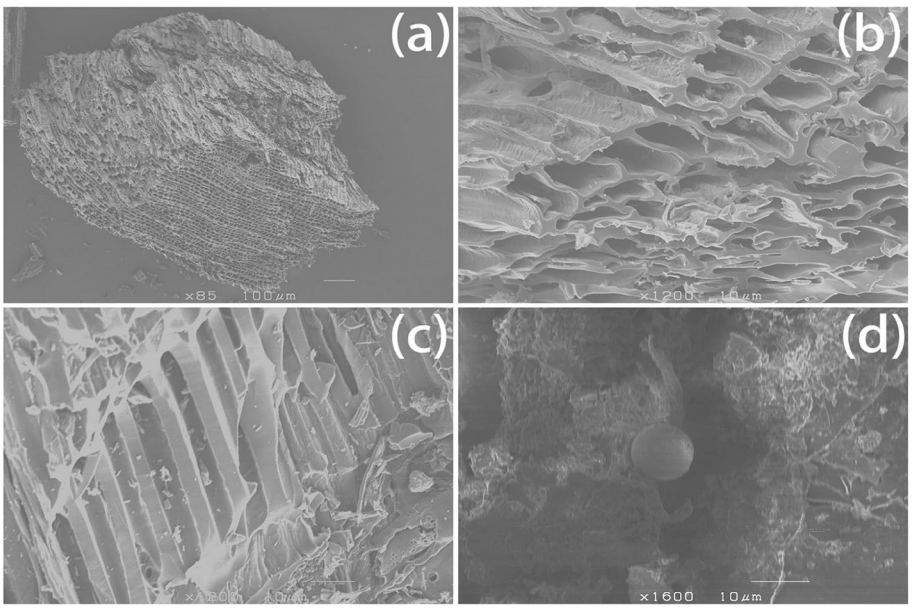

Fig. 6 Structure of biochar from wood chips of conifer. All photographs were taken by SEM: **a** Biochar granules (85 ×); **b** Pore structure at cutoff (350 ×); **c** Fence-like structure inside (1200 ×); **d** Structure within the internal voids of biochar after 100 days of AD (1600 ×)

Table 4 The characteristics of biochar before and after AD

Parameter	Biochar before AD	Biochar after AD
pH	8.85	8.59
Electrical conductivity (mS cm^{-1})	0.62	3.67
Ash (%)	19.64	12.57
C (%)	76.93	78.02
N (%)	0.52	0.96
Nitrate nitrogen (mg L^{-1})	4.2	5.2
Ammonia nitrogen (mg L^{-1})	16	184
P (%)	0.09	0.32
Ca (%)	1.22	1.10
Mg (%)	0.22	0.34
K (%)	0.47	0.74
Mn (%)	328.60×10^{-4}	246.09×10^{-4}
Zn (%)	73.74×10^{-4}	89.07×10^{-4}
Cu (%)	14.35×10^{-4}	13.95×10^{-4}
Fe (%)	0.34	0.31
Ni (%)	20.51×10^{-4}	31.48×10^{-4}
Co (%)	8.67×10^{-4}	10.85×10^{-4}

Data given on dry matter basis

involved in the methanogenic pathway of acetate fragmentation [33]. Likewise, K, Ca, and Mg are essential for the growth and development of some methanogenic bacteria and are crucial for the formation of microbial aggregates. Therefore, the presence of these elements in biochar may explain the enhanced effect of biochar addition on the performance of AD processes. After use in AD processing, the concentration of ammonia nitrogen in biochar increased significantly from 16 to 184 mg L^{-1}, indicating that biochar addition had the effect of capturing ammonia nitrogen.

3.3.2 Changes in biochar mineralogical composition and functional groups

The crystal structure of biochar before and after AD was investigated by XRD. The camel peak (~ 20°) in the diffractogram was cellulose crystals [34]. The raw biochar showed very little crystallinity. In the biochar samples after AD, the peaks at 20.8°, 26.6° and 45.7° are characteristic peaks of quartz (Qtz). The peak observed at 28.3° and 40.5° probably corresponds to the precipitation of sylvite (Syl). The presence of calcite (Cal) was prominently found in both biochars before and after AD (Fig. 7a), which is consistent with the high Ca content found in elemental analysis (Table 4). Overall, after AD, the diffraction peaks of Qtz, Cal and Syl were sharper and more intense, indicating that these highly crystalline properties were produced, and crystalline phases of potassium salt (KCl) are common in biochars. Since the biochar has higher surface area and active sites, the amorphous components generated provide a potential buffer capacity to acids formed during AD [35].

ATR-FTIR spectra of biochar before and after AD showed many broad overlapping peaks between 1700 and 600 cm^{-1} (Fig. 7b), indicating the presence of minerals and organic matters. The broad band around 1089 cm^{-1} may be caused by P-containing functional groups, such as P-O bonds of phosphates [36], which are beneficial for the growth of anaerobic bacteria. Both organic (phosphoric acid mono and diesters) and inorganic (orthophosphates and their oligomers) phosphates [37] can also contribute to the strong belt. Other inorganic components, such as sulfates and silicates [36], contribute to the strong peaks at 970–1200 cm^{-1}, and corresponded to the Qtz crystal structure from XRD analysis. The peak in this region of 1025 cm^{-1} band is attributed to the symmetric C-O stretching of cellulose, hemicellulose and lignin. Carboxylic acids, aldehydes, etc. in biochar could act as energy sources for selected microorganisms [38]. The presence of additional phenolic C-O and carboxylic -COO stretching bands with high absorption intensity in biochar after AD indicates that its alkalinity is lower than that of raw biochar because phenolic functional groups promote acidity in biochar [39]. Furthermore, the presence of oxygen-containing functional groups in biochar after AD suggests its relatively more hydrophilic character, possibly representing a better ability to adsorb organic compounds [40]. Therefore, the absorbance intensities of the mentioned functional groups in biochar increased after AD. Overall, as a kind of sustainable material with great potential in AD process, biochar shows the excellent functionality (fine pore structure, abundant inorganic metal salts and basic functional groups).

4 Conclusions

In long-term anaerobic co-digestion of FW with CG with continuous feeding, the digestion was greatly inhibited by the accumulation of VFAs and ammonia nitrogen. Re-inoculation restored the methanogenic capacity during the first five phases (each phase with 10 days) by raising the pH. However, in the subsequent experimental phase, re-inoculation could not reverse reactor imbalance and eventually resulted in process failure. Biochar addition was a favorable action for improving AD performance

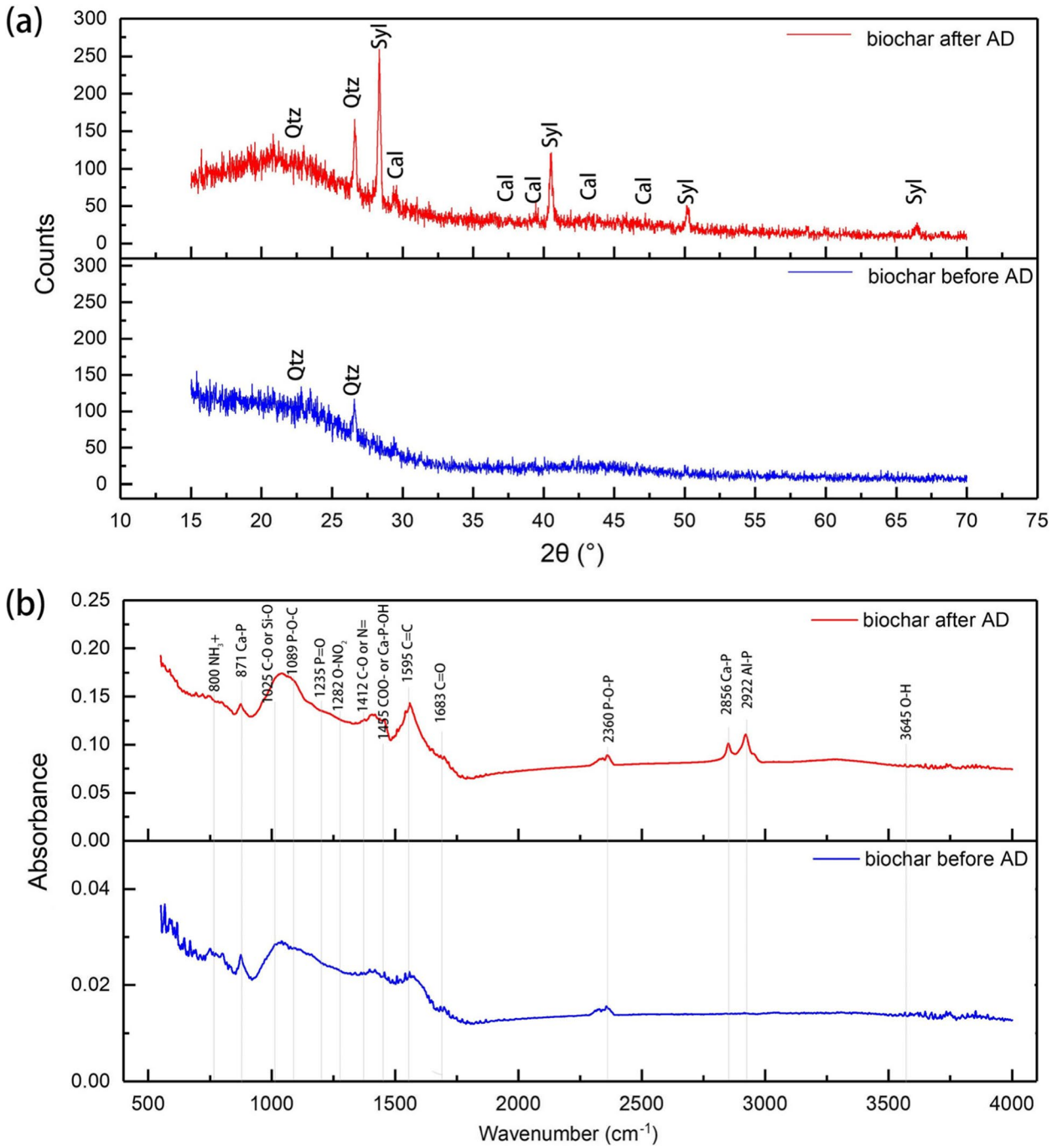

Fig. 7 XRD patterns (**a**) of biochars before and after AD. Peaks of quartz (Qtz), calcite (Cal), sylvite (Syl) in XRD spectra are designated, and FTIR-ATR spectra (**b**) of biochars before and after AD. Major peaks of different functional groups are indicated

by accelerating the conversion of macromolecular substances to dissolved substrates and increasing the buffering capacity. The BA treatment achieved the highest cumulative methane yield of 5.80 NL and avoided the inhibitory effect of high VFAs and ammonia nitrogen concentration in the digestate. The results indicate that the use of biochar in AD processes will contribute to process sustainability.

Acknowledgements
The determination of biochar properties was performed by the Tokachi Federation of Agricultural Cooperatives. Scanning electron microscopy analysis was conducted with the support of the Electron Microscope Laboratory, Research Faculty of Agriculture, Hokkaido University. We are also grateful to the Global Facility Center and Faculty of Engineering Technical Center of Hokkaido University for conducting FTIR and XRD analyses.

Authors' contributions
X.L. and N.S. contributed to the design and implementation of the research, the analysis of the results, and the writing of the manuscript. N.S. verified the analytical methods and supervised the findings of this work. All authors have read and approved the final manuscript.

Funding
This work was supported by the Japan Science and Technology Agency (JST) through a SPRING grant (Support for Pioneering Research Initiated by the Next Generation, Grant Number: JPMJSP2119).

Availability of data and materials
All data generated or analyzed during this study are provided in the submitted article.

Declarations

Competing interests
The authors declare they have no competing interests.

Received: 12 September 2022 Accepted: 28 January 2023
Published online: 07 February 2023

References

1. Xu FQ, Li YY, Ge XM, Yang LC, Li YB. Anaerobic digestion of food waste–Challenges and opportunities. Bioresource Technol. 2018;247:1047–58.
2. Yoshida K, Kametani K, Shimizu N. Adaptive identification of anaerobic digestion process for biogas production management systems. Bioproc Biosyst Eng. 2020;43:45–54.
3. Hutnan M, Kolesarova N, Bodik I. Anaerobic digestion of crude glycerol as sole substrate in mixed reactor. Environ Technol. 2013;34:2179–87.
4. Li XJ, Shimizu N. Effects of lipase addition, hydrothermal processing, their combination, and co-digestion with crude glycerol on food waste anaerobic digestion. Fermentation. 2021;7:284.
5. Bouallagui H, Touhami Y, Cheikh RB, Hamdi M. Bioreactor performance in anaerobic digestion of fruit and vegetable wastes. Process Biochem. 2005;40:989–95.
6. Zhang B, Zhang LL, Zhang SC, Shi HZ, Cai WM. The influence of pH on hydrolysis and acidogenesis of kitchen wastes in two-phase anaerobic digestion. Environ Technol. 2005;26:329–39.
7. Meng XS, Yu DW, Wei YS, Zhang YX, Zhang QF, Wang ZY, et al. Endogenous ternary pH buffer system with ammonia-carbonates-VFAs in high solid anaerobic digestion of swine manure: an alternative for alleviating ammonia inhibition? Process Biochem. 2018;69:144–52.
8. Li LH, Li D, Sun YM, Ma LL, Yuan ZH, Kong XY. Effect of temperature and solid concentration on anaerobic digestion of rice straw in South China. Int J Hydrogen Energ. 2010;35:7261–6.
9. Fdez-Guelfo LA, Alvarez-Gallego CJ, Marquez DS, Garcia LIR. Destabilization of an anaerobic reactor by wash-out episode: effect on the biomethanization performance. Chem Eng J. 2013;214:247–52.
10. Wu LJ, Kobayashi T, Kuramochi H, Li YY, Xu KQ. Recovery strategies of inhibition for mesophilic anaerobic sludge treating the de-oiled grease trap waste. Int Biodeter Biodegr. 2015;104:315–23.
11. Feng K, Wang Q, Li H, Zhang YY, Deng Z, Liu JG, et al. Effect of fermentation type regulation using alkaline addition on two-phase anaerobic digestion of food waste at different organic load rates. Renew Energ. 2020;154:385–93.
12. Masebinu SO, Akinlabi ET, Muzenda E, Aboyade AO. A review of biochar properties and their roles in mitigating challenges with anaerobic digestion. Renew Sust Energ Rev. 2019;103:291–307.
13. Wang JL, Wang SZ. Preparation, modification and environmental application of biochar: a review. J Clean Prod. 2019;227:1002–22.
14. Elbeshbishy E, Nakhla G. Batch anaerobic co-digestion of proteins and carbohydrates. Bioresource Technol. 2012;116:170–8.
15. APHA. Standard methods for the examination of water and wastewater. 19th ed. Washington, DC: American Public Health Association; 1995.
16. Tipson RS. Infrared spectroscopy of carbohydrates. Washington, DC: United States Department of Commerce, National Bureau of Standards; 1968.
17. Feng SS, Hou SX, Huang X, Fang Z, Tong YJ, Yang HL. Insights into the microbial community structure of anaerobic digestion of municipal solid waste landfill leachate for methane production by adaptive thermophilic granular sludge. Electron J Biotechn. 2019;39:98–106.
18. Li Y, Chen YG, Wu J. Enhancement of methane production in anaerobic digestion process: a review. Appl Energ. 2019;240:120–37.
19. Yin CK, Shen YW, Yuan RX, Zhu NW, Yuan HP, Lou ZY. Sludge-based biochar-assisted thermophilic anaerobic digestion of waste-activated sludge in microbial electrolysis cell for methane production. Bioresource Technol. 2019;284:315–24.
20. Shen YW, Linville JL, Ignacio-de Leon PAA, Schoene RP, Urgun-Demirtas M. Towards a sustainable paradigm of waste-to-energy process: enhanced anaerobic digestion of sludge with woody biochar. J Clean Prod. 2016;135:1054–64.
21. Li DJ, Song LY, Fang HL, Li P, Teng Y, Li YY, et al. Accelerated biomethane production rate in thermophilic digestion of cardboard with appropriate biochar: dose-response kinetic assays, hybrid synergistic mechanism, and microbial networks analysis. Bioresource Technol. 2019;290:121782.
22. Yuan JH, Xu RK, Zhang H. The forms of alkalis in the biochar produced from crop residues at different temperatures. Bioresource Technol. 2011;102:3488–97.
23. Li Q, Liu YQ, Yang XH, Zhang JW, Lu B, Chen R. Kinetic and thermodynamic effects of temperature on methanogenic degradation of acetate, propionate, butyrate and valerate. Chem Eng J. 2020;396:125366.
24. Xu CX, Ding YY, Liu JC, Huang WW, Cheng QP, Fan GZ, et al. Anaerobic digestion of sulphate wastewater mediated by biochar. Environ Technol. 2021;1–12. https://doi.org/10.1080/09593330.2021.2011428.
25. Ma JY, Pan JT, Qiu L, Wang Q, Zhang ZQ. Biochar triggering multipath methanogenesis and subdued propionic acid accumulation during semi-continuous anaerobic digestion. Bioresource Technol. 2019;293:122026.
26. Fidel RB, Laird DA, Thompson ML, Lawrinenko M. Characterization and quantification of biochar alkalinity. Chemosphere 2017;167:367–73.
27. Hale SE, Alling V, Martinsen V, Mulder J, Breedveld GD, Cornelissen G. The sorption and desorption of phosphate-P, ammonium-N and nitrate-N in cacao shell and corn cob biochars. Chemosphere. 2013;91:1612–9.
28. Yenigun O, Demirel B. Ammonia inhibition in anaerobic digestion: a review. Process Biochem 2013;48:901–11.
29. Fagbohungbe MO, Herbert BMJ, Hurst L, Ibeto CN, Li H, Usmani SQ, et al. The challenges of anaerobic digestion and the role of biochar in optimizing anaerobic digestion. Waste Manage. 2017;61:236–49.
30. Shaaban A, Se SM, Dimin MF, Juoi JM, Husin MHM, Mitan NMM. Influence of heating temperature and holding time on biochars derived from rubber wood sawdust via slow pyrolysis. J Anal Appl Pyrol. 2014;107:31–9.
31. Pan JT, Ma JY, Liu XX, Zhai LM, Ouyang XH, Liu HB. Effects of different types of biochar on the anaerobic digestion of chicken manure. Bioresource Technol. 2019;275:258–65.
32. Vintiloiu A, Boxriker M, Lemmer A, Oechsner H, Jungbluth T, Mathies E, et al. Effect of ethylenediaminetetraacetic acid (EDTA) on the bioavailability of trace elements during anaerobic digestion. Chem Eng J. 2013;223:436–41.
33. Romero-Guiza MS, Vila JJ, Mata-Alvarez J, Chimenos JM, Astals S. The role of additives on anaerobic digestion: a review. Renew Sust Energ Rev. 2016;58:1486–99.

34. Yu F, Li XM, Wang JT, Wang XT, Xiao H, Wang Z, et al. Coupling anaerobic digestion with pyrolysis for phosphorus-enriched biochar production from constructed wetland biomass. Acs Sustain Chem Eng. 2022;10:3972–80.
35. Tchomgui-Kamga E, Alonzo V, Nanseu-Njiki CP, Audebrand N, Ngameni E, Darchen A. Preparation and characterization of charcoals that contain dispersed aluminum oxide as adsorbents for removal of fluoride from drinking water. Carbon. 2010;48:333–43.
36. Wen B, Zhang JJ, Zhang SZ, Shan XQ, Khan SU, Xing BS. Phenanthrene sorption to soil humic acid and different humin fractions. Environ Sci Technol. 2007;41:3165–71.
37. Jiang W, Saxena A, Song B, Ward BB, Beveridge TJ, Myneni SCB. Elucidation of functional groups on gram-positive and gram-negative bacterial surfaces using infrared spectroscopy. Langmuir 2004;20:11433–42.
38. Sharma B, Suthar S. Enriched biogas and biofertilizer production from *Eichhornia* weed biomass in cow dung biochar-amended anaerobic digestion system. Environ Technol Inno 2021;21:101201.
39. Lopez-Ramon MV, Stoeckli F, Moreno-Castilla C, Carrasco-Marin F. On the characterization of acidic and basic surface sites on carbons by various techniques. Carbon. 1999;37:1215–21.
40. Inyang M, Gao B, Pullammanappallil P, Ding WC, Zimmerman AR. Biochar from anaerobically digested sugarcane bagasse. Bioresource Technol. 2010;101:8868–72.

Publisher's Note